Kinetics of particle wrapping by a vesicle

Stephen Mirigian and Murugappan Muthukumar[a)]
Department of Polymer Science and Engineering, University of Massachusetts, Amherst, Massachusetts 01003, USA

(Received 22 March 2013; accepted 30 June 2013; published online 25 July 2013)

We present theoretical results on kinetics for the passive wrapping of a single, rigid particle by a flexible membrane. Using a simple geometric ansatz for the shape of the membrane/particle complex we first compute free energy profiles as a function of the particle size, attraction strength between the particle and vesicle, and material properties of the vesicle—bending stiffness and stretching modulus. The free energy profiles thus computed are taken as input to a stochastic model of the wrapping process, described by a Fokker-Planck equation. We compute average uptake rates of the particle into the vesicle. We find that the rate of particle uptake falls to zero outside of a thermodynamically allowed range of particle sizes. Within the thermodynamically allowed range of particle size, the rate of uptake is variable and we compute the optimal particle size and maximal uptake rate as a function of the attraction strength, the vesicle size, and vesicle material properties. © *2013 AIP Publishing LLC*. [http://dx.doi.org/10.1063/1.4813921]

I. INTRODUCTION

The wrapping of a particle by a fluid membrane is a phenomenon of widespread and generic interest in biology[1–4] as well as in a variety of technological applications such as drug delivery,[5–12] gene delivery,[13,14] and the design of nanoreactors[15–24] which would allow for highly controllable reaction conditions.

While the diversity of systems, materials, and mechanisms of particle wrapping is wide, certain generic physical features of the process are inescapable. Dietrich and coworkers[25] made steps towards elucidating these features by studying the adhesion of latex spheres to "giant lipid vesicles" with sizes in the range of 10–100 μm. Using light microscopy they observed through time four steps in the passive engulfment of the latex bead: adhesion, ingestion, expulsion, and recapture. They were able to model the observed behavior with a simple, single parameter, geometric model that accounted only for the interplay between membrane tension and the adhesion energy between the vesicle and bead. Deserno and Gelbart[26] subsequently extended this model with the addition of a second parameter, considering the balance of membrane curvature, tension, and adhesion. This allowed them to predict the behavior of smaller bead sizes, an inadequacy of the earlier theory. Using this model they constructed a phase diagram for the equilibrium degree of wrapping in terms of the relative size of the vesicle and the particle. A key finding was the importance of a softened "shoulder" in the neighborhood of the adhered particle allowing for the passage of much smaller beads than in the earlier model of Dietrich *et al.*[25]

In the related problem of uptake of macromolecules by membranes, Wang and Muthukumar have recently computed the free energy for a polyelectrolyte chain inside a rigid spherical cavity.[27] They have found that for sufficiently large attractive energies between the chain and the confining membrane there exists an optimal size of the vesicle dictated by the balance between chain confinement and attractive interactions. When the attractive energy is lowered, this energy dominated regime crosses over to an entropy dominated regime, wherein the optimal size of the confining cavity becomes infinite.

We consider here the complementary problem to that of Wang and Muthukumar:[27] the wrapping of a rigid bead by a flexible vesicle. We consider the vesicle to possess a bending and stretching modulus and to wrap the rigid particle while maintaining a constant internal volume. We find that the bending and stretching moduli of the membrane dictate a range of particle sizes over which wrapping will occur, with an intermediate particle size at which the rate of wrapping is maximized. The ability to design synthetic vesicles able to uptake soft particles such as a polymer will rely on the ability to match the energy scales, material properties, and length scales of the vesicle to those of the particle.

In the remainder of the paper, we compute the kinetics of passage rate using a simple geometrical ansatz for the vesicle shape. In Sec. II we introduce the geometrical model used to compute free energy profiles, following the work of Deserno and Gelbart.[26] We then introduce the Fokker-Planck formalism which enables us to compute passage rates for these free energy profiles. In Sec. III we show results for the free energy landscapes and their associated passage rates, optimal particle sizes, and maximum passage rates as a function of the relative sizes of the vesicle and bead and as a function of vesicle material properties. Finally, we close with brief concluding remarks in Sec. IV.

II. MODEL

A. Geometry

We model the encapsulation of a rigid spherical particle by a fluid membrane using the geometrical ansatz shown in

a)Author to whom correspondence should be addressed. Electronic mail: muthu@polysci.umass.edu

 © 2013 AIP Publishing LLC

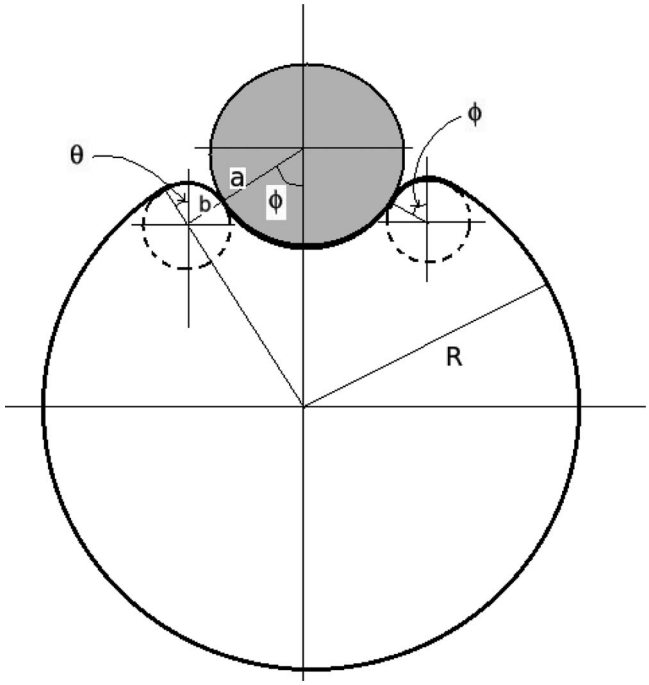

FIG. 1. Geometry of the particle-vesicle complex.

Fig. 1. Our geometrical model is originally due to Deserno and Gelbart[26] and so it is necessary to briefly recapitulate their discussion. At any given point in the process of encapsulation, we assume the membrane will have three sections, which we call the contact region, the shoulder region, and the bulk region. The contact region is defined by the surface of contact between the soft vesicle and the rigid spherical particle. The radius of the spherical particle is a in Fig. 1. The angle defined by the line joining the center of the vesicle and bead and the line between the center of the sphere and the point at which the bead and the vesicle are no longer in contact is defined to be ϕ. In our model, the angle ϕ is the order parameter defining the degree of wrapping. When the particle is completely unwrapped and only just tangentially in contact with the vesicle ϕ will be zero. When the particle is fully wrapped, we will have $\phi = \pi$. Intermediate values of ϕ represent partial stages of wrapping. The model does not incorporate the rupture of the vesicle wall as the final stage. Deserno and Gelbart[26] have previously shown that for certain parameters of the model (discussed below), a partially wrapped state will be the global free energy minimum, and therefore the equilibrium value of ϕ will lie somewhere in the range $[0, \pi]$. The bulk of the vesicle we take to be spherical with radius R. The contact region and bulk region are joined by a rounded shoulder, which we assume follows the contour of a toroid from an angle $-\theta$ to the angle ϕ. The inner radius of the toroidal shoulder is defined to be b. Examination of Fig. 1 shows that the outer radius of the toroidal region can be either using the parameters a, b, and ϕ, or using θ and R. This implies the relation $(a + b)\sin(\phi) = (R - b)\sin(\theta)$. It follows that we may take θ as determined by a, b, ϕ, and R and not as an independent parameter of the model.

A well known result from the geometry of surfaces states that a sphere encloses a maximum volume with the minimum possible surface area.[28] This result suggests a definition of the excess area of a closed vesicle in the following way.[26] Define a radius, R_0, which is prescribed by the initial volume enclosed by the vesicle according to $V_0 = 4/3\pi R_0^3$. The lipids (or other material) making up the vesicle will, in equilibrium, preferentially span an area A_{eq}, provided they are under no tension. The excess area of the vesicle will be given by the difference between this preferred area and the area of a sphere with radius R_0: $A_{ex} = A_{eq} - 4\pi R_0^2$. If $A_{ex} > 0$ the relaxed membrane will have more area than necessary to enclose its volume and will therefore be flaccid. In this regime, the deviation from our model geometry is large and the full shape equations[29–31] must be solved numerically to arrive at an accurate understanding of the complexation. However, if $A_{ex} < 0$ then the membrane will be under tension and take a spherical shape with radius R_0. It is in this regime that the assumption of a spherical bulk region and toroidal shoulder region will be most accurate.

During the process of encapsulation of a rigid spherical bead by a closed vesicle, as in Fig. 1, the resistance of a vesicle membrane to bending and stretching must be overcome by the free energy gain in the system due to adhesion of the bead to the membrane. Although there are several equilibrium shapes[31] for a vesicle, we consider only the simplest spherical shape for the vesicle in the present study. Assuming that the energies due to adhesion, bending, and stretching are additive (ignoring nonlinear coupling among these), the free energy will therefore be a sum of the adhesion energy, the bending penalty, and the stretching penalty,[31]

$$\Delta F = -wA_{contact} + \frac{\kappa}{2}\int_{\Omega}(2H - c_0)^2 + \lambda\frac{\Delta A^2}{2A_0}, \qquad (1)$$

where w, κ, and λ are the energy penalty (or gain) for adhesion, bending, and stretching, respectively.

The first term on the right-hand side of Eq. (1) gives the attractive energy between the rigid particle and the vesicle membrane, which we take to be proportional to the area of contact between them. In the problem of Wang and Muthukumar[27] involving the interaction between a polyelectrolyte and a rigid sphere, reasonable physical values for the attractive energy at high salt concentrations are $w \approx 0.1\text{–}1 k_B T/\text{nm}^2$, depending on the charge density of the surface and polymer, salt valency, and solvent properties. Although charged systems present many additional complexities,[32] our geometric model described above will be a reasonable approximation to the true membrane shape at high salt concentrations.

Additionally, Dietrich and Angelova obtained a similar value of $w \approx 0.25 k_B T/\text{nm}^2$ in an uncharged system in their experiments with latex spheres being wrapped by "giant lipid vesicles."[25]

The second term on the right-hand side of Eq. (1) gives the bending energy as harmonic in the mean curvature as the well known Helfrich free energy.[33] H is the mean curvature of the membrane for a given vesicle geometry, given by $H = 1/2(1/r_1 + 1/r_2)$, where r_1 and r_2 are the principal radii at a point on the surface. The spontaneous curvature, c_0, is constant at all points on the vesicle and is a property of the membrane that arises from asymmetry in the areas of the inner and outer leaflets of a lipid bilayer.[33–35] This asymmetry then

induces a curvature in the membrane even in the absence of external forces. The bending energy is then with reference to this spontaneous curvature. The bending modulus is typically of the order of $10k_BT$, although experimentally measured values vary somewhat. A review of typical experimental techniques and reported values is given by Marsh.[36]

The third term on the right-hand side of Eq. (1) is the stretching free energy penalty. We take this to be harmonic in the change of the vesicle area $\Delta A = A - A_0$, where $A_0 = 4\pi R_0^2$ is the initial area of the vesicle and A is the area of the vesicle for a given geometry determined by a, b, R, and ϕ. We take λ, the membrane stretching modulus, to be near $50k_BT$, which is the measured value for 1-stearoyl-2-oleoyl-phosphatidylcholine lipid bilayers.[37]

Using the ansatz of Fig. 1, we can compute analytical expression for the contact, bending, and stretching contributions based on the differential geometry of the surface. The contact adhesion energy is simply proportional to the area of the contact region between the vesicle and the bead. This can be calculated in a straightforward way as

$$F_{ad}^{cont} = -w\int dA^{cont} = -2\pi\int_0^{\phi} d\phi' a^2 \sin\phi' = -2\pi w a^2(1-\cos\phi). \tag{2}$$

In order to calculate the contribution to the free energy from bending, we must compute the Helfrich free energy given in Eq. (1) for each region of the vesicle. In the contact region, we obtain

$$F_b^{cont} = \kappa\int dA^{cont}(H-c_0)^2 = 2\pi\kappa a^2(1-\cos\phi)\left(\frac{1}{a}-c_0\right)^2, \tag{3}$$

where we have used $H = 1/a$ for a sphere of radius a and c_0 is a spontaneous curvature. The bending penalty for the toroidal region is

$$F_b^{tor} = \kappa\int dA^{tor}(2H-c_0)^2 \times\frac{\pi}{2}\kappa b\left[\int_{-\theta}^{\phi} d\psi\frac{\sin^2\psi}{(a+b)\sin\phi - b\sin\psi} + 2(\cos\theta-\cos\phi)\left(\frac{1}{b}+c_0\right) + [(a+b)(\theta+\phi)\sin(\phi)+b(\cos\theta-\cos\phi)]\left(\frac{1}{b}+c_0\right)^2\right]. \tag{4}$$

The bending energy of the bulk region is

$$F_b^{bulk} = 2\pi\kappa R^2\left(\frac{1}{R}-c_0\right)^2(1+\cos\theta). \tag{5}$$

The stretching energy penalty at a given wrapping angle is taken to be harmonic in the change of area, as given by Eq. (1).

Likewise, we must calculate the area of the vesicle geometry, which is the sum of the areas of the contact, toroidal, and bulk region, in order to know the stretching contribution to the free energy. These areas are given by

$$A^{cont} = 2\pi a^2(1-\cos\phi), \tag{6a}$$

$$A^{tor} = 2\pi b[(a+b)\sin\phi(\theta+\phi) + b(\cos(\theta)+\cos(\phi))], \tag{6b}$$

$$A^{bulk} = 2\pi R^2(1+\cos(\theta)). \tag{6c}$$

Inserting these expressions pertaining to the geometry of the complex into Eq. (1), we arrive at an expression for the free energy of the complex as a function of the wrapping angle ϕ, inner radius of the toroidal shoulder b, and radius of the bulk region R:

$$\begin{aligned}\mathcal{F}[\phi,b] = {} & -2\pi w a^2(1-\cos\phi) + 2\pi\kappa a^2(1-\cos\phi)\left(\frac{1}{a}-c_0\right)^2 \\ & +\pi\kappa\left\{\frac{b}{2}\int_{-\theta}^{\phi} d\psi\frac{\sin^2\psi}{(a+b)\sin\phi - b\sin\psi}\right. \\ & +b\left(\frac{1}{b}+c_0\right)(\cos\theta-\cos\phi) \\ & +\frac{b}{2}\left(\frac{1}{b}+c_0\right)^2[(\theta+\phi)(a+b)\sin\phi + b(\cos\theta-\cos\phi)] \\ & \left.+2R^2\left(\frac{1}{R}-c_0\right)^2(1+\cos\theta)-4\right\} \\ & +2\pi\lambda\left\{a^2(1-\cos\phi) + b[(a+b)\sin\phi(\theta+\phi)\right. \\ & \left.+b(\cos\phi-\cos\theta)] + R^2(1+\cos\theta) - 2R_0^2\right\}^2/R_0^2.\end{aligned} \tag{7}$$

Here, θ is not independent, but is related to R, b, a, and ϕ by the relation $(a+b)\sin\phi = (R-b)\sin\theta$ as described above. Because the particle being wrapped is rigid, its radius a is a physical parameter of the problem and does not change throughout the process of wrapping, as is also true of the adhesion energy w and the membrane moduli κ and λ.

We assume that wrapping occurs at a fixed internal volume of the vesicle, so that R is determined by the constraint

$$\begin{aligned}\Delta V = {} & \frac{4}{3}\pi R_0^3 - \left\{\frac{2}{3}\pi R^3(1+\cos\theta) - \frac{2}{3}\pi a^3(1-\cos\phi)\right. \\ & +\frac{1}{3}\pi(a+b)^2\sin^2\phi[(R-b)\cos\theta + (a+b)\cos\phi] \\ & \left.+\pi b^2\left[(\theta+\phi)(1+b)\sin\phi + \frac{2}{3}b(\cos\phi-\cos\theta)\right]\right\} \\ = {} & 0.\end{aligned} \tag{8}$$

Using this equality, R is eliminated from Eq. (7) so that the free energy of the complex is a function of ϕ and b only, as indicated by the notation $\mathcal{F}[\phi, b]$ in Eq. (7). At a fixed value of the wrapping angle ϕ, this free energy is a function only of the inner radius b of the toroidal shoulder, and (for that given ϕ) will have a minimum at a value of the toroid radius $b = b^*(\phi)$.

By minimizing the free energy with respect to b at each value of ϕ, we eliminate b from Eq. (7) so that the free energy is a function of the wrapping angle only, $F(\phi) = \mathcal{F}[\phi, b^*(\phi)]$. In writing the free energy in this way, we assume that the inner radius of the toroid changes smoothly and the wrapping process is slow enough to allow the vesicle conformation to relax to this minimum free energy shape as the wrapping angle changes.

Dietrich and Angelova[25] have previously examined a similar free energy, neglecting the curvature effects of the membrane and assuming that the wrapping process is dictated entirely by the balance between adhesion energy and stretching of the membrane and can be characterized by two dimensionless parameters. One is defined as $\zeta = w/\lambda$, the ratio of the material constants in the problem, and the second is the ratio of the bead radius to the vesicle radius, a/R_0, characterizing the geometry of the bead/vesicle complex. For the case of a large particle being wrapped, the toroidal shoulder is relatively small and the bending contribution to the free energy is negligible in comparison to the stretching necessary to encapsulate the particle. Introduction of curvature effects, as by Deserno and Gelbart[26] and as we have done here, quantifies this approximation by introducing a natural length scale into the problem, $l_c = \sqrt{\kappa/w}$. For particles much larger than this length scale, bending effects will be negligible and the wrapping process is well described by the model of Dietrich and Angelova,[25] controlled by the dimensionless parameter ζ and the ratio of bead radius to vesicle radius. However, when the particle radius is of the order of l_c, curvature effects become an important contribution to the free energy landscape.

By examining the limit of the free energy as the particle is fully wrapped, with $\phi \to \pi$, Deserno and Gelbart[26] used thermodynamic arguments to show that there exists a minimum vesicle size necessary in order to wrap a particle of radius a. They give an estimate of this minimum size by

$$R_0\sqrt{\zeta}/l_c = \frac{a/l_c}{\sqrt{2 - 4.603(l_c/a)^2}}. \tag{9}$$

They point out that this expression diverges for a particle radius a where the denominator vanishes. At this particle radius, the minimum size of the vesicle becomes infinite so that there is no vesicle size which can wrap particles smaller than this size, given by

$$a_{min} \approx 1.52 l_c. \tag{10}$$

The value of this minimum radius is controlled entirely by l_c, depending on the adhesion strength and the bending modulus while being insensitive to the stretching modulus. Further, they suggest that the wrapping of large particles is controlled primarily by stretch in the membrane, characterized by the dimensionless parameter $\sqrt{\zeta}$ from Eq. (9). They conclude that at small particle sizes wrapping behavior is dictated entirely by bending of the membrane, while at large particle sizes wrapping is dictated by stretching of the membrane.

B. Kinetics

At a given wrapping angle, we assume that thermal fluctuations of the membrane causes the area of contact between the bead and vesicle to change in a stochastic way throughout the process of wrapping, so that ϕ can be treated as a random variable moving from 0 to π with some drift due to the free energy gradient in Eq. (7). Drawing an analogy with nucleation theory,[38] we define the probability of the membrane being wrapped to angle ϕ at time t to be $W(\phi, t)$. At any given time, the probability that the wrapping angle will transition to some different wrapping angle at $\phi \pm d\phi$ will obey a master equation:

$$\frac{\partial}{\partial t}W(\phi,t) = k_{\phi-d\phi}W(\phi - d\phi, t) - k'_{\phi}W(\phi,t) - k_{\phi}W(\phi,t) + k'_{\phi+d\phi}W(\phi + d\phi, t). \tag{11}$$

Here, k_ϕ is the transition rate between a wrapping angle ϕ to an incrementally larger wrapping angle $\phi + d\phi$, while k'_ϕ is the transition rate in the other direction, from ϕ to $\phi - d\phi$. Invoking detailed balance $k'_{\phi+d\phi}$ can be written in terms of k_ϕ so that in the continuous limit we obtain[39]

$$\frac{\partial}{\partial t}W(\phi,t) = \frac{\partial}{\partial \phi}\left[\frac{k}{k_B T}\frac{\partial F(\phi)}{\partial \phi}W(\phi,t) + k\frac{\partial}{\partial \phi}W(\phi,t)\right], \tag{12}$$

where we have additionally assumed that the transition rate $k_\phi \equiv k$ is constant throughout the wrapping process. k sets a fundamental time scale for the stochastic process of wrapping and is determined by nonuniversal features of the membrane such as the relaxation of the small lipids and other microscopic details of the wrapping. The mapping of the wrapping process to the Fokker-Planck equation makes the important assumption that the encapsulation process is slow compared to the relaxation of the small lipid molecules within the membrane, so that the vesicle equilibrates fully at each wrapping angle. If this assumption does not hold, memory effects in the membrane will become important and our approach needs to be modified.

Viewing the wrapping angle as a stochastic variable means that the encapsulation of the particle will occur over a distribution of times, related to the full probability distribution, $W(\phi, t)$.[40] The average time at which the wrapping angle first equals π (full encapsulation) is defined to be the mean first passage time and is given by

$$\tau = \int_0^\infty dt\, t\dot{W}(\phi, t). \tag{13}$$

The mean first passage time can be shown to obey the equation (related to the backward Fokker-Planck equation)[40]

$$\frac{k}{k_B T}\frac{\partial F(\phi_0)}{\partial \phi_0}\frac{\partial}{\partial \phi_0}\tau(\phi_0) + k\frac{\partial^2}{\partial \phi_0^2}\tau(\phi_0) = -1. \tag{14}$$

Assuming that the particle does not disengage the vesicle complex during the process of encapsulation, this equation can be solved to give an expression for the mean first passage time of the particle into the vesicle as[40]

$$\tau = \frac{1}{k}\int_0^{2\pi} d\phi_1 \int_0^{\phi_1} d\phi_2 e^{[F(\phi_1) - F(\phi_2)]/k_B T}. \tag{15}$$

Our primary quantity of interest is the uptake rate of the particle which we define to be the inverse of the mean first

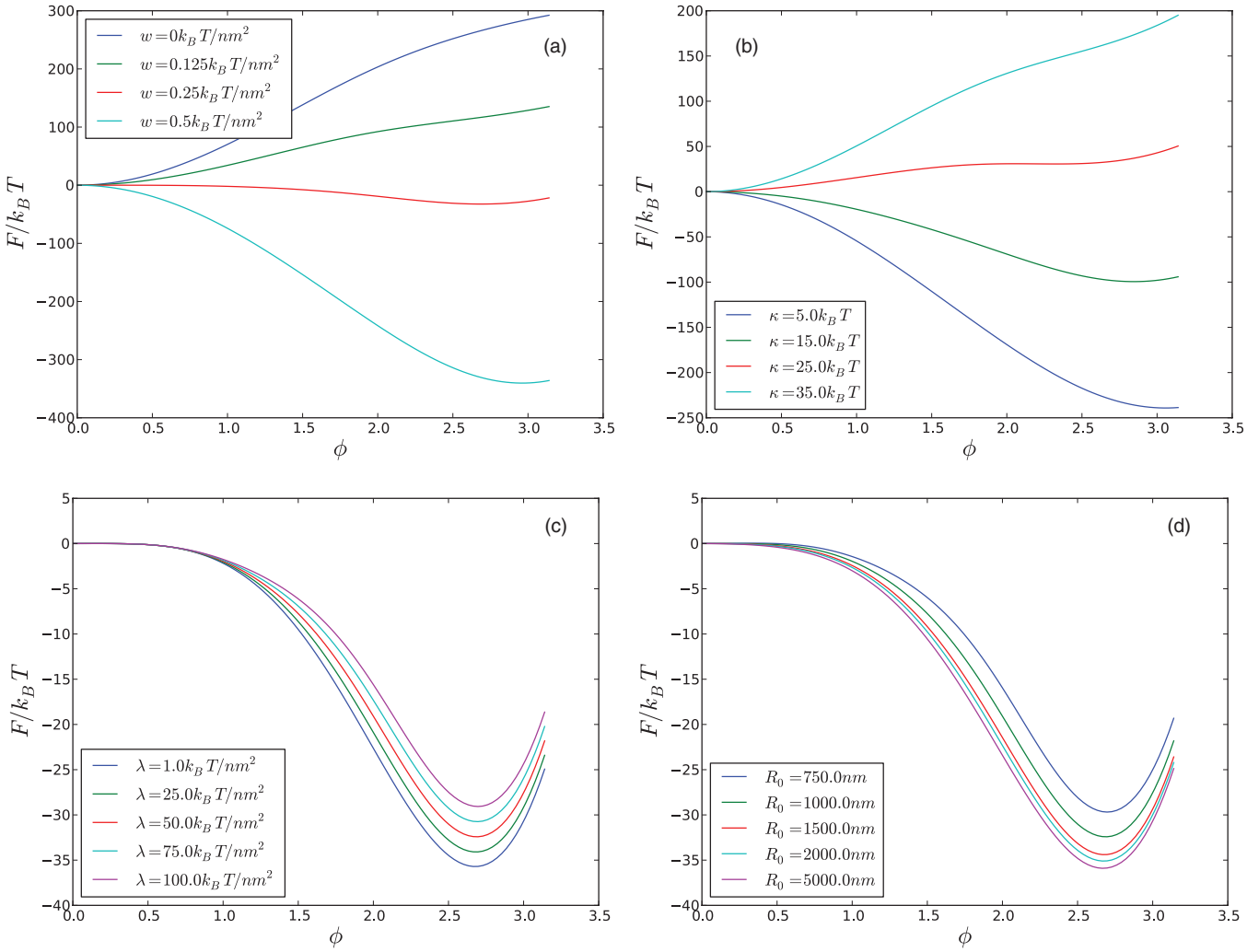

FIG. 2. Free energy landscapes for a small particle, $a = 10$ nm. (a) $R_0 = 1\ \mu$m, $\kappa = 20\ k_BT$, $\lambda = 50\ k_BT$. (b) $R_0 = 1\ \mu$m, $w = 0.25\ k_BT/\text{nm}^2$, $\lambda = 50\ k_BT/\text{nm}^2$. (c) $R_0 = 1\ \mu$m, $w = 0.25\ k_BT/\text{nm}^2$, $\kappa = 20\ k_BT$. (d) $w = 0.25\ k_BT/\text{nm}^2$, $\kappa = 20\ k_BT$, $\lambda = 50\ k_BT/\text{nm}^2$.

passage time, $1/\tau$. We wish to understand how the adhesion between the particle and the vesicle, the bending and stretching moduli of the vesicle, and particle and vesicle sizes affect this quantity.

III. RESULTS

We organize our results by first presenting explicit free energy landscapes, illustrating the differing effects of the adhesion energy, material constants of the vesicle, and vesicle size on the wrapping of a small and a large particle. We then directly show the effect of varying the particle size over a range of values. Using these free energy landscapes we then show passage rates for vesicles of differing size, adhesion energies, and material constants as a function of particle size. In keeping with the thermodynamic arguments of Deserno and Gelbart[26] we find a non-zero uptake rate only within a range of particle sizes, dictated by the characteristics of the vesicle. Within the range of particle sizes that will be fully wrapped by a vesicle of given size, adhesion strength, and material properties, we find that there is a maximal uptake rate which occurs for a particle of optimum size.

A. Free energy landscapes

A typical set of free energy landscapes over ϕ are shown in Figs. 2 and 3. All plots in Fig. 2 show a typical set of free energy landscapes for a small particle, $a = 10$ nm, while all plots in Fig. 3 are for a large particle with $a = 75$ nm. The size of the vesicle in these figures is taken to be 1 μm. Within each figure, the insets have been arranged for easy comparison between them, so that, e.g., Fig. 2(a) is comparable to Fig. 3(a), save for a different bead size and so on for each figure. Our findings here are in keeping with previous results of Deserno and Gelbart,[26] although here we have presented explicit free energy landscapes. We have done this to elucidate several features of the free energy landscape.

In both Figs. 2(a) and 3(a) we see that for small attractive energies w, between the vesicle and particle, the free energy is a minimum at $\phi = 0$, indicating that the particle will remain completely unwrapped. As the attractive energy is increased, the fully wrapped $\phi = \pi$ state becomes the equilibrium configuration. At intermediate strengths of the attractive interaction the global minimum occurs at an intermediate value of ϕ, indicating that a partially wrapped state is the equilibrium configuration. The depth of this intermediate minimum

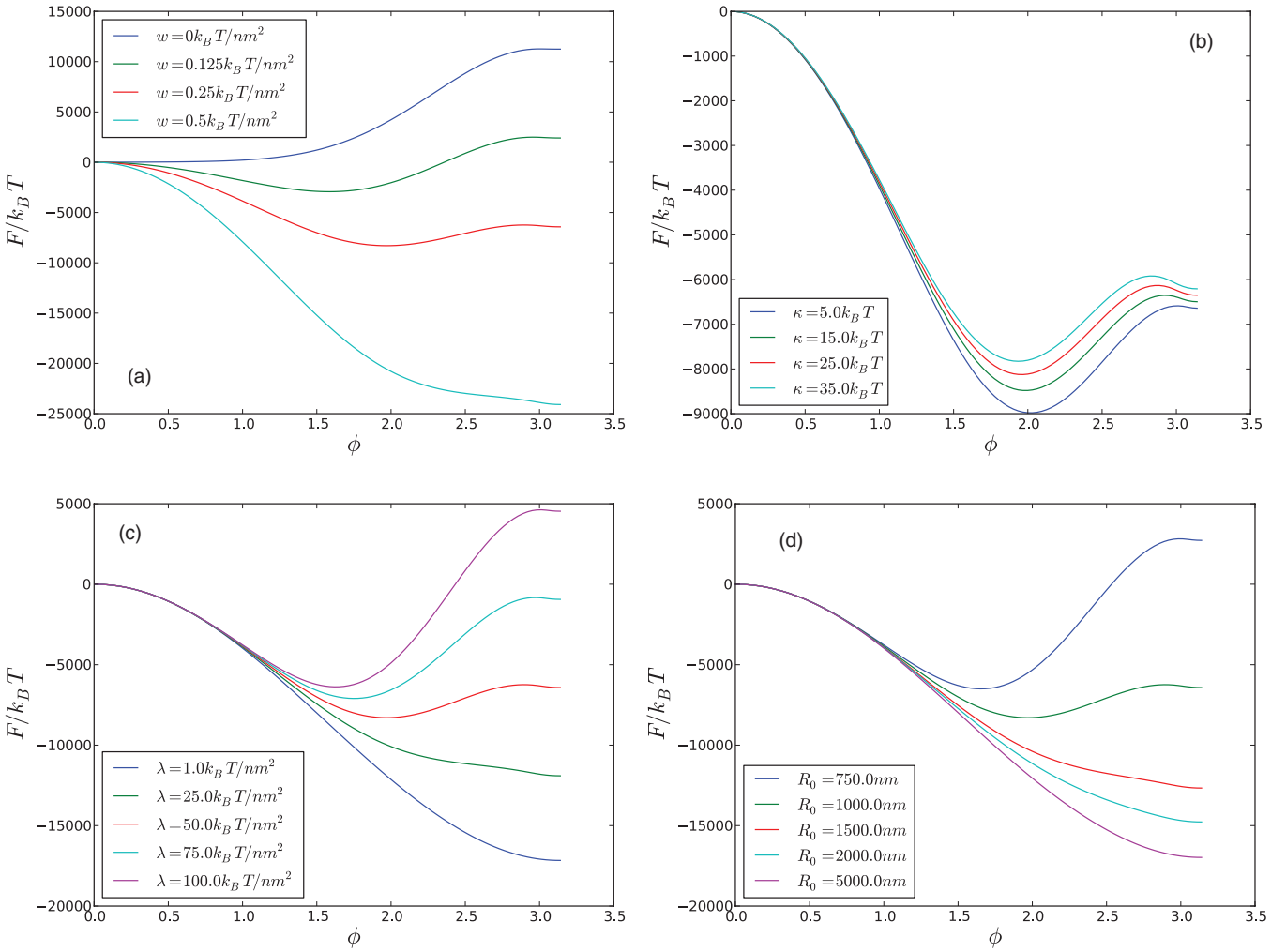

FIG. 3. Free energy landscapes for a large particle, $a = 75$ nm. (a) $R_0 = 1\,\mu$m, $\kappa = 20\ k_BT$, $\lambda = 50\ k_BT/\text{nm}^2$. (b) $R_0 = 1\,\mu$m, $w = 0.25\ k_BT/\text{nm}^2$, $\lambda = 50\ k_BT/nm^2$. (c) $R_0 = 1\,\mu$m, $w = 0.25\ k_BT/\text{nm}^2$, $\kappa = 20\ k_BT$. (d) $w = 0.25\ k_BT/\text{nm}^2$, $\kappa = 20\ k_BT$, $\lambda = 50\ k_BT/\text{nm}^2$.

is much shallower for the small particle shown in Fig. 2(a), in keeping with expression (2), which shows that the attractive energy is a function not only of the adhesion strength but also of the area of contact. A larger bead presents a larger area of contact, resulting in the deeper minimum in Fig. 3(a).

Figs. 2(b) and 3(b) show the effect of changes in the bending modulus on the free energy landscape for small (Fig. 2(b)) and large (Fig. 3(b)) particles. In contrast to changes in the adhesion energy, which effected a transition from unwrapped to fully wrapped equilibrium states for both particle sizes, changes in the bending modulus of the membrane have only a muted effect on the free energy landscape for large particle sizes and a typical range of experimental bending moduli,[36] shown in Fig. 3(b). For the small particle size, shown in Fig. 2(b), decreasing the bending modulus results in a transition from an equilibrium unwrapped state (e.g., for $\kappa = 35k_BT$) to an equilibrium wrapped state (e.g., for $\kappa = 5k_BT$). The marked difference in the effect of changing the bending modulus for different particle sizes is consistent with the previous discussion of the length scale l_c, which arises in the limit of small particles. When $a \gg l_c$, κ does not significantly affect the free energy. This can be further intuitively justified by considering that Eqs. (3) and (5) are (when $c_0 = 0$) independent of the bead size, while Eq. (4) goes like a. Thus, the bending contribution to the free energy only increases linearly with increasing particle size. Equations (2) and (6) show that the adhesion and stretching energies increase with particle size like a^2. Thus, for small particle size, the bending contribution to the free energy is significant, and therefore changing the bending modulus has a significant effect on the free energy landscape. For large particle sizes bending is still present, but the adhesion and stretching contributions dominate the bending contribution.

The effect of membrane stretching is in contrast to this behavior due to the bending of the membrane, and can be seen by comparing Figs. 2(c) and 2(d) to Figs. 3(c) and 3(d). These figures show the effects of changing the stretching modulus and initial vesicle size for a small particle in Fig. 2 and a large particle in Fig. 3. The stretching modulus and the vesicle size are analogous to one another in that they both control the stretching contribution to the free energy landscape for a fixed particle size. At a small particle size, shown in Fig. 2, the overall stretching penalty is small, and changing the initial vesicle size or the stretching modulus has only a small effect on the overall free energy landscape, as can be seen in Figs. 2(c) and 2(d), respectively. In contrast, the

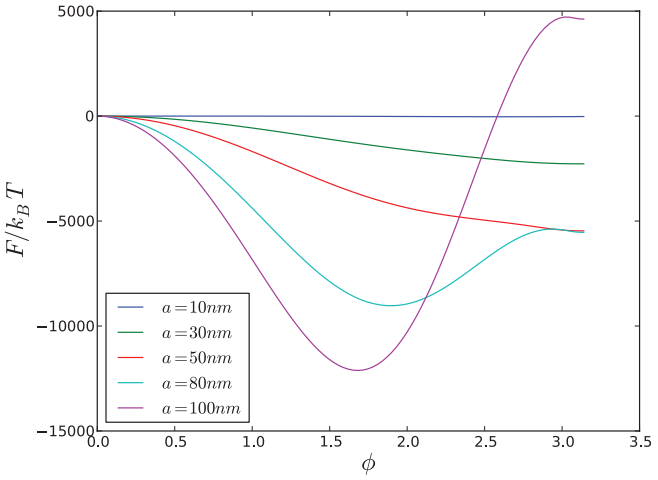

FIG. 4. Free energy landscape with $R_0 = 1\,\mu$m, $w = 0.25\,k_BT/\text{nm}^2$, $\kappa = 20\,k_BT$, $\lambda = 50\,k_BT/\text{nm}^2$.

necessary area change of the membrane needed in order to engulf a large particle while maintaining a constant volume is large. Because of this, changes to the stretching contribution lead to very different free energy landscapes for a large particle, shown in Figs. 3(c) and 3(d). Comparison of Figs. 3(c) and 3(d) shows that an increase in the stretching modulus is analogous to shrinking the initial size of the vesicle. From Eq. (9) Deserno and Gelbart[26] argued that as the stretching modulus is increased, the equilibrium state of the complex changes from a fully wrapped to a partially wrapped state. Stretching of the membrane is very small at small wrapping angles, and partial wrapping is forbidden only in the limit of an infinitely stiff vesicle. An increase in the stretching contribution to the free energy, whether via a decrease of the initial particle size or an increase in the stretching modulus, will never completely forbid at least some minimal partial wrapping for suitable values of the adhesion energy and particle size.

This change in the profile of the free energy in going from small particles to larger particle sizes is illustrated explicitly in Fig. 4 where we have plotted the free energy as a function of ϕ for various particle sizes ranging from $a = 10$ nm to $a = 100$ nm, holding all other features of the system constant. As we have just discussed, at small particle sizes, increasing the particle size increases the area of contact between the particle and vesicle, increasing the contact energy between them. For a 1 μm vesicle with $w = 0.25\,k_BT/\text{nm}^2$, $\kappa = 20\,k_BT$, and $\lambda = 50\,k_BT/\text{nm}^2$ shown in Fig. 4, this is seen by comparing the blue curve for $a = 10$ nm, which will remain completely unwrapped to the green curve for $a = 30$ nm, which will be completely wrapped due to the greater adhesion energy from the great contact area with the larger particle. As the size of the particle is further increased from, e.g., $a = 50$ nm to $a = 80$ nm, the stretching energy due to the area change necessary to fully encapsulate the particle causes the free energy of the fully wrapped state to become large and a minimum forms in the free energy at an intermediate wrapping angle. The equilibrium configuration of the complex is partially wrapped. Previous work by Deserno and Gelbart has

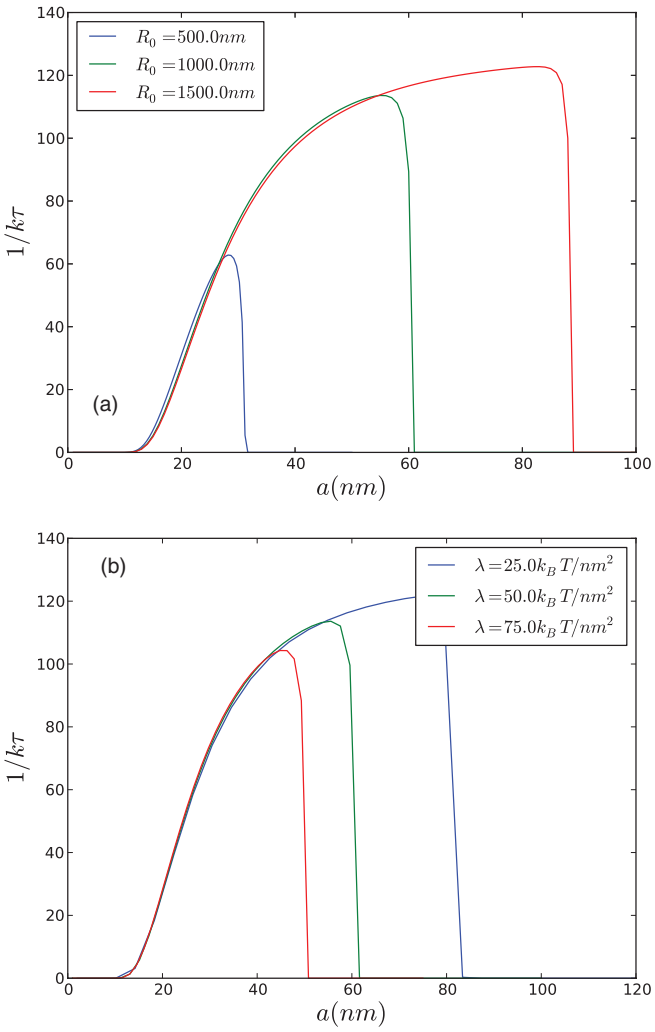

FIG. 5. Uptake rate for changing vesicle size and stretching modulus. (a) R_0 with $w = 0.25\,k_BT/\text{nm}^2$, $\kappa = 20\,k_BT$, $\lambda = 50\,k_BT/\text{nm}^2$. (b) $R_0 = 1\,\mu$m, $w = 0.25\,k_BT/\text{nm}^2$, $\kappa = 20\,k_BT$.

mapped the phase diagram for differing vesicle/bead sizes[26] and differing stretching and adhesion energies.[29]

B. Kinetics of wrapping

We use free energy profiles such as those shown in Figs. 2–4 to compute uptake rates from Eq. (15). Fig. 5 shows the effect of vesicle size and stretching modulus on the uptake rate of particles. The uptake rate is non-zero only within a range of particle sizes, defining a range of selectivity of the vesicle. As an illustrative example, at a particle size of $a = 10$ nm, the uptake rate shown in Fig. 5(a) is zero for all vesicle sizes. For a vesicle size of 1 μm, this corresponds to the blue curve in Fig. 4, which monotonically increases and shows a minimum at $\phi = 0$, giving a completely unwrapped equilibrium configuration. Choosing now $a = 50$ nm, Fig. 5(a) shows an uptake rate of $1/k\tau \approx 100$. This uptake rate corresponds to the red free energy profile shown in Fig. 4 for $a = 50$ nm. Further increase in the size of the particle leads to a sharp dropoff in the uptake rate to zero, corresponding to the appearance of a partially wrapped minimum in the free energy

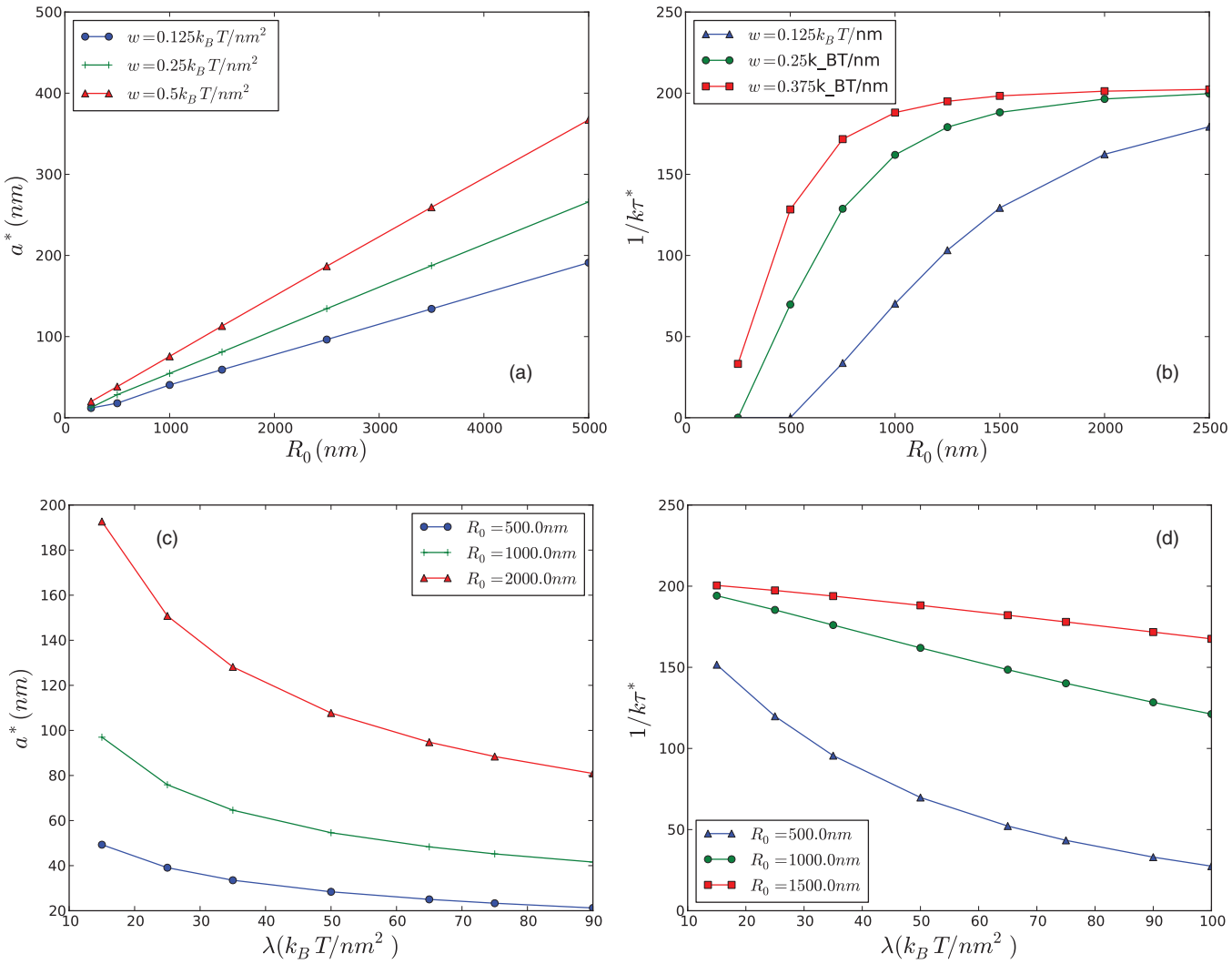

FIG. 6. Optimal particle sizes and associated maximal uptake rates as a function of vesicle size and stretching modulus. (a) $\kappa = 20\ k_BT$, $\lambda = 50\ k_BT/\text{nm}^2$. (b) $\kappa = 20\ k_BT$, $\lambda = 50\ k_BT/\text{nm}^2$. (c) $w = 0.25\ k_BT/\text{nm}^2$, $\kappa = 20\ k_BT$. (d) $w = 0.25\ k_BT/\text{nm}^2$, $\kappa = 20\ k_BT$.

profile of Fig. 4. The sharpness of this dropoff is a function of the large values of the free energy involved, of the order of $10^5\ k_BT$. Thus, the depth of the free energy minimum increases beyond 1 k_BT very quickly with further increases in the size of the particle. The sharpness of the dropoff means that the range of allowed particle sizes that will become fully wrapped corresponds closely to those particle sizes previously computed by Deserno and Gelbart.[26] As expected from the above discussion of the free energy landscapes, we see that only the upper limit of this allowed range is controlled by these two features of the complex. This arises because the stretching contribution to the free energy enters primarily for large particle sizes. The wrapping for small particles is controlled primarily by the balance between bending and adhesion energies, and is therefore not affected by the vesicle size or the stretching modulus.

The uptake rates in Fig. 5 show a maximum at a particle size which we define as a^* with a corresponding uptake rate $1/\tau^*$. The optimum particle size lies close to the upper cutoff particle size, and therefore is largely controlled by this boundary. As discussed above, this implies that it is largely controlled by the onset of the intermediate minimum in the free energy profile due to an increase in the stretching penalty for wrapping larger particles. In Fig. 6(a) we show this optimal particle size as a function of vesicle size. We find that a^* grows linearly with R_0, with a slope controlled by the strength of the attractive energy. For $w = 0.125$ we find $a^* = 0.038R_0$, $w = 0.25$ gives $a^* = 0.053R_0$, and $w = 0.5$ gives $a^* = 0.072R_0$. The competition between stretching and adhesive energies can be characterized by the ratio of the adhesive energy and the stretching modulus[25] as discussed above. We find that increasing the vesicle size increases the optimal particle size with a slope roughly given by $\sqrt{\zeta} = \sqrt{w/\lambda}$ so that $a^* \sim \sqrt{\zeta} R_0$. This is a direct consequence of a^* being determined primarily by the stretching penalty and the sharp cutoff in the uptake rate in Fig. 5 and was previously reported by Deserno and Gelbart[26] with reference to the maximum allowable particle size. It is important to emphasize that in principle the maximum allowable size for encapsulation and the optimum size can be quite different, as is the case for some biological model of endocytosis emphasizing diffusion of membrane receptors.[11] This picture is also consonant with the behavior of a^* as λ is increased. Fig. 6(b) shows a^* falling off $\sim 1/\sqrt{\lambda}$, in keeping with this relationship.

The presence of an optimal particle size corresponds with a maximal uptake rate for particles of that size, which we have defined to be $1/\tau^*$. In Figures 6(b) and 6(d), we have plotted this maximal uptake rate as a function of vesicle size and stretching modulus, respectively. As an example, we take $w = 0.25\ k_BT$ in Fig. 6(a) and see that the vesicle will preferentially uptake particles with a radius of ∼75 nm. This corresponds in Fig. 6(b) to a maximal uptake rate of $1/\tau^* \approx 175$ in units of the rate constant, k. It is important to realize that each data point in Fig. 6(b) (and Figures 6(d), 8(b), and 8(d)) is computed for a different size of the particle, and therefore has a unique free energy landscape associated with it. For this reason, analytical results are not available. From this free energy landscape (chosen to maximize the uptake rate), we have computed $1/\tau^*$ via Eq. (15).

Fig. 6(b) shows that below a certain minimum size of the vesicle, all uptake of particles is inhibited; i.e., for $w = 0.25\ k_BT$ this is near $R_0 = 250$ nm. This lower limit on vesicle size arises because of an interplay between the attractive energy and stretching energy. As has been previously discussed, the attractive energy driving wrapping is proportional to the area of contact between the particle and the vesicle so that in order for the particle to be wrapped by the membrane, it must be large enough that the attractive energy creates a negative slope in the free energy. However, small vesicles have a great sensitivity to increasing particle size, as even small increases in particle size necessitate large stretching energies to wrap. At some minimum initial size of the vesicle, the particle size necessary to drive the downhill attractive force creates a stretching penalty too large to allow full wrapping, and the uptake rate falls to zero. Increasing R_0 above this minimum vesicle size initially leads to a rapid increase in uptake rate. As the vesicle size is further increased, the uptake rate ceases to be significantly affected by the stretching penalty and further increases in the vesicle size do not increase the maximal uptake rate.

When the stretching modulus is increased it has the inverse effect to that of increasing the vesicle size, as was previously seen through the relation $a^* \sim \sqrt{\zeta}R_0$. Thus, increasing $1/\sqrt{\lambda}$ has the same effect as increasing R_0. This is seen in Fig. 6(d), where decreasing the stretching modulus decreases the stretching penalty for wrapping, increasing the uptake rate in an analogous way to that discussed above for increasing vesicle size. At a sufficiently large stretching modulus, the uptake rate would drop to zero. However, we have not included these points as these values are beyond those seen in typical experimental systems.[37]

In Fig. 7 we have plotted uptake rates as a function of particle size for various attractive energies and bending moduli of the membrane. In contrast to the uptake rate curves shown in Fig. 5, manipulation of the bending modulus of the membrane controls size selectivity by moving the lower particle size limit towards larger particles, shown in Fig. 7(a). Thus, a vesicle with bending modulus $\kappa = 5\ k_BT$ has a minimum particle radius of near 7 nm, in agreement with the estimate $1.52l_c = 6.79$ nm provided by Deserno and Gelbart.[26] Changing the bending modulus to $\kappa = 60\ k_BT$ gives a minimum particle size of 29 nm against $1.52l_c = 23.5$ nm and $\kappa = 90\ k_BT$ gives a minimum particle size of 40 nm against a corresponding estimate of $1.52l_c = 29$ nm. This difference between the estimate of minimum particle size from the phase diagram and that predicted by the uptake kinetics serves to emphasize that the selectivity of particle sizes predicted by the uptake kinetics is not identical with the phase diagram boundaries. Although significantly smaller particles are predicted to bind to the vesicle in equilibrium, the rate of uptake will be vanishingly slow. Nonetheless, the general feature in Fig. 7(a) is that the selectivity is controlled through the bending modulus mainly by excluding smaller particles from uptake and different bending moduli will have little effect on the upper size limit of particles that can be wrapped. As with uptake curves shown in Fig. 5, the uptake curves for different bending moduli, shown in Fig. 7(a), show a sharp dropoff near the maximum particle size, originating from the same formation of an intermediate minimum in the free energy landscapes of Fig. 4 as discussed above. The position of the optimum particle size (corresponding to the maximum in uptake rate) is quite close to this maximal particle size.

Fig. 7(b) shows the uptake rate as a function of particle size for a fixed vesicle size at varying values of the

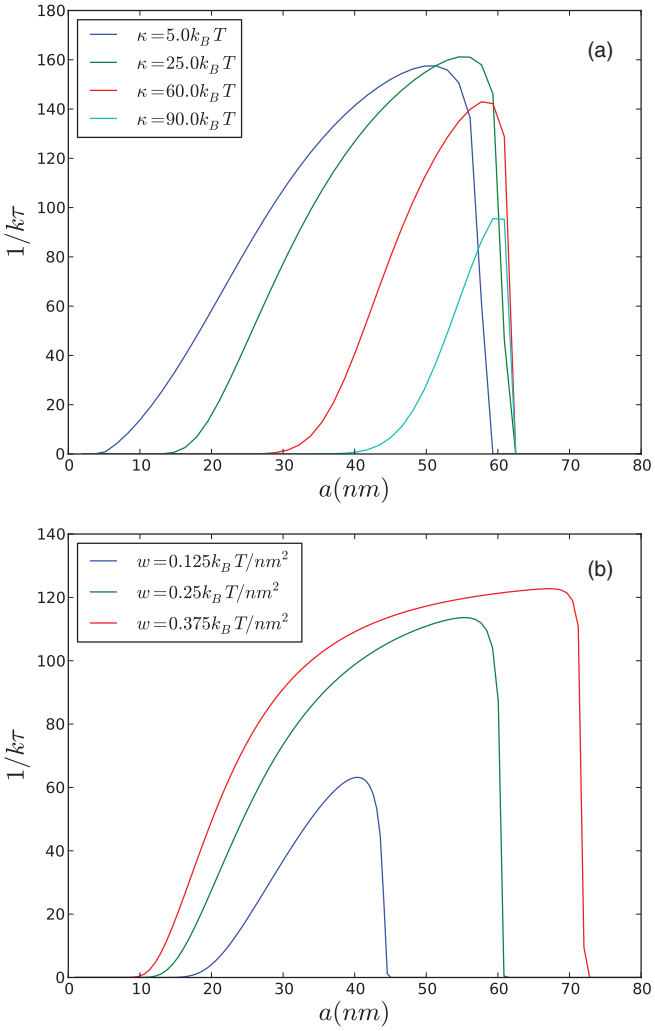

FIG. 7. Uptake rate for bending and stretching modulus. (a) $R_0 = 1\ \mu$m, $w = 0.25\ k_BT/\text{nm}^2$, $\lambda = 50\ k_BT/\text{nm}^2$. (b) $R_0 = 1\ \mu$m, $\kappa = 20\ k_BT$, $\lambda = 50\ k_BT/\text{nm}^2$.

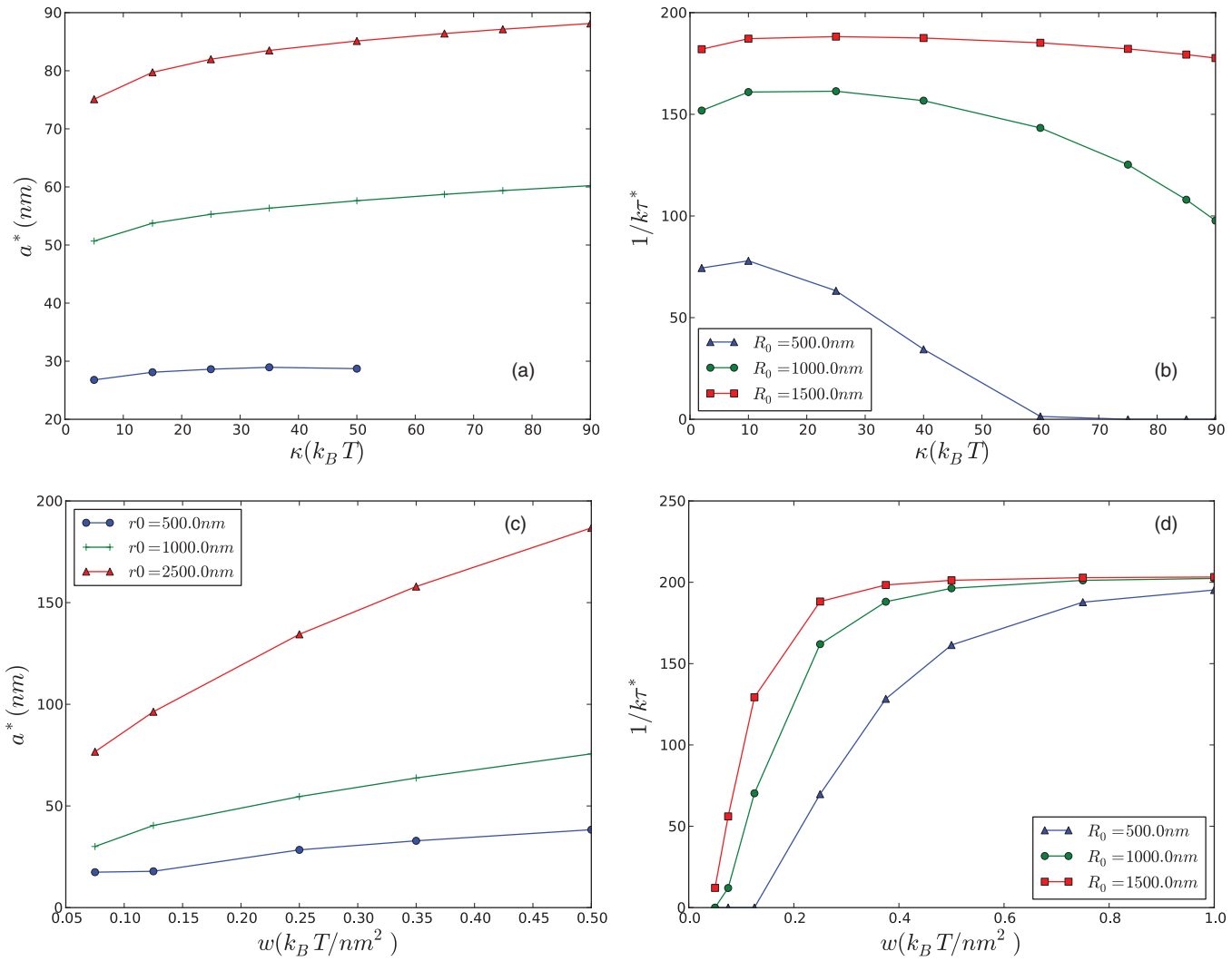

FIG. 8. Optimal particle radius and associated maximal uptake rates for various vesicle sizes as a function of the bending modulus and attractive energy. (a) $w = 0.25\ k_BT/\text{nm}^2$, $\lambda = 50\ k_BT/\text{nm}^2$. $R_0 = 0.5\ \mu$m (blue circles), 1 μm (green crosses), 1.5 μm (red triangles). (b) $w = 0.25\ k_BT/\text{nm}^2$, $\lambda = 50\ k_BT/\text{nm}^2$. (c) $\kappa = 20\ k_BT$, $\lambda = 50\ k_BT/\text{nm}^2$. (d) $\kappa = 20\ k_BT$, $\lambda = 50\ k_BT/\text{nm}^2$.

adhesion energy. The adhesion energy is the driving force for wrapping of both small and large particles, characterized by $l_c = \sqrt{\kappa/w}$ and $\zeta = w/\lambda$, respectively. In keeping with this observation, we see that both the upper and lower limits on particle size are controlled by changes in the adhesion energy. Again examining the lower bound on particle size for $w = 0.125\ k_BT/\text{nm}^2$ we see that the uptake rate will vanish for $a \approx 10$ nm, against an estimate of $1.52l_c = 19.2$ nm. Likewise, for $w = 0.375\ k_BT/\text{nm}^2$, the uptake rate vanishes below $a = 17$ nm while $1.52l_c = 11.1$ nm. At maximal particle sizes, the estimate provided by $\sqrt{\zeta}R_0$ follows the trend of increasing with increasing w as well. The uptake curves again show the sharp dropoff after the optimal particle as a consequence of the onset of an intermediate minimum with increasing particle size, as shown in Fig. 4 and discussed above. We note that the adhesion energy is unique in controlling the selectivity of particle size by excluding *both* upper and lower allowable particle sizes, whereas all other features of the system – i.e., vesicle size, bending modulus, and stretching modulus – control either the upper or the lower limit alone.

The uptake rates plotted in Fig. 7 show a maximum with increasing particle size, which we defined above to be a^*, with a corresponding maximal uptake rate, which is defined as $1/\tau^*$. Fig. 8 shows these optimal particle sizes and maximal uptake rates as functions of the bending modulus and adhesion strength. In Fig. 8(a) the optimal particle size is plotted against the bending modulus. As previously observed, the optimal particle size follows the trend of the maximum allowable particle size due to the extremely sharp dropoff in the uptake rate as an intermediate minimum is formed in the free energy. Because the bending modulus has only a minimal effect on the uptake of a large particle, the change in the optimal particle size is correspondingly weak. However, the maximal uptake rate in Fig. 8(b) shows a marked dependence on the bending modulus, falling off smoothly to zero with increasing bending modulus. For sufficiently large κ, all uptake will be prohibited. This occurs for a 0.5 μm vesicle at a bending stiffness of 60 k_BT, for example. This behavior can be rationalized from the plot of uptake kinetics in Fig. 7(a). As the bending modulus increases, the lower allowed particle size increases in a manner roughly proportional to $l_c = \sqrt{\kappa/w}$, while the

maximal allowed particle size does not change, not being controlled by the bending modulus. Eventually, the bending modulus can be made stiff enough that l_c is of the same order of $\sqrt{\zeta}R_0$ (the quantity controlling the upper cutoff), and the range of allowed particle sizes goes to zero. It is noteworthy that the Fokker-Planck formalism predicts that this falloff occurs smoothly and is not simply a sudden dropoff. This allows for the possibility to tune the properties of a membrane in order to optimize particle size selectivity and uptake rate over a range of rates, and not simply tune the system to wrap or not wrap a particle in a binary way.

Fig. 8(c) shows the optimal particle size as a function of the adhesion energy. In keeping with the above discussion, the optimal particle size follows closely with the maximal allowed particle size, which increases like $\sqrt{\zeta}R_0 \sim \sqrt{w}R_0$. The corresponding maximal uptake rate as a function adhesion energy is shown in Fig. 8(d). Clearly, as expected, below some value of the adhesion energy, no uptake will occur. Increasing the adhesion energy initially leads to a rapid increase in uptake rate, which tapers off at larger and larger values of w. At large values of the adhesion energy, the wrapping process occurs so quickly that the incremental increase in adhesion energy does not proportionally increase the speed of the wrapping process.

IV. CONCLUSION

We have used a minimal model based on geometric considerations to compute the kinetics of wrapping a particle by a vesicle. Within this range of allowed particle sizes we have found an optimum particle size, which we have called a^*, at which the uptake rate is maximized. The maximum uptake rate can be manipulated by changing the properties of the membrane such as bending stiffness, stretching modulus, size of the vesicle, and adhesion energy between the vesicle and particle. We find that the increase of the stretching modulus or bending stiffness slows down the rate of uptake smoothly to zero. Increasing adhesion energy or the vesicle size increases uptake rate smoothly only up to a point, beyond which additional increases in these parameters have a diminishing effect.

The wrapping process is largely controlled by the interplay between adhesion energy of the particle to the vesicle and the bending and stretching penalties from changing the geometry. On the basis of these competing factors, we find that the material properties of the membrane dictate a range of particle size which can be wrapped by the membrane. Particles with sizes outside this range will not be wrapped, consistent with previous thermodynamic equilibrium theories. The lower particle size limit is controlled by the adhesion between the particle and the membrane and the bending stiffness of the membrane and is independent of the stretching modulus or size of the vesicle. An upper limit on the particle size is controlled by the stretching modulus of the membrane (or, equivalently, the size of the vesicle).

The extension of the present work to the encapsulation of charged macromolecules is of interest, with the additional necessity to account for conformational entropy of the macromolecule. This is relegated to a future publication.

ACKNOWLEDGMENTS

The authors acknowledge the National Science Foundation (Grant No. 1105029) and the National Institutes of Health (Grant No. R01HG002776), and the Materials Research Science and Engineering Center at the University of Massachusetts Amherst.

[1] *Endocytosis*, edited by M. Marsh (Oxford University Press, 2001).
[2] *Endocytosis*, edited by I. Pastan and M. C. Willingham (Plenum Press, New York, NY, 1985).
[3] M. Marsh, Biochem. J. **218**, 1 (1984).
[4] A. E. Smith and A. Helenius, Science **304**, 237 (2004).
[5] H. Gao, W. Shi, and L. B. Freund, Proc. Natl. Acad. Sci. U.S.A. **102**, 9469 (2005).
[6] X. Li and D. Xing, Appl. Phys. Lett. **97**, 153704 (2010).
[7] B. D. Chithrani and W. C. W. Chan, Nano Lett. **7**, 1542 (2007).
[8] H. Yuan, J. Li, G. Bao, and S. Zhang, Phys. Rev. Lett. **105**, 138101 (2010).
[9] L. M. Bareford and P. W. Swaan, Adv. Drug Delivery Rev. **59**, 748 (2007).
[10] Z. M. Qian, H. Li, H. Sun, and K. Ho, Pharmacol. Rev. **54**, 561 (2002).
[11] S. Zhang, J. Li, G. Lykotrafitis, G. Bao, and S. Suresh, Adv. Mater. **21**, 419 (2009).
[12] J. Ziello, Y. Huang, and I. S. Jovin, Mol. Med. **16**, 222 (2010).
[13] A. V. Korobko, C. Backendorf, and J. R. C. van der Maarel, J. Phys. Chem. B **110**, 14550 (2006).
[14] A. V. Korobko, W. Jesse, and J. R. C. van der Maarel, Langmuir **21**, 34 (2005).
[15] K. A. Smith, D. Jasnow, and A. C. Balazs, J. Chem. Phys. **127**, 084703 (2007).
[16] C. S. Peyratout and L. Dähne, Angew. Chem. **43**, 3762 (2004).
[17] C. Gao, S. Leporatti, S. Moya, E. Donath, and H. Möhwald, Langmuir **17**, 3491 (2001).
[18] A. A. Antipov and G. B. Sukhorukov, Adv. Colloid Interface Sci. **111**, 49 (2004).
[19] A. Gómez-Hens and J. M. Fernández-Romero, Trends Analyt. Chem. **24**, 9 (2005).
[20] W. N. Vreeland and L. E. Locascio, Anal. Chem. **75**, 6906 (2003).
[21] A. Karlsson, M. Karlsson, R. Karlsson, S. Kristin, A. Lundqvist, M. Tokarz, and O. Orwar, Anal. Chem. **75**, 2529 (2003).
[22] J. W. Hong and S. R. Quake, Nat. Biotechnol. **21**, 1179 (2003).
[23] Y.-C. Tan, K. Hettiarachchi, M. Siu, Y.-R. Pan, and A. P. Lee, J. Am. Chem. Soc. **128**, 5656 (2006).
[24] E. S. Lee, D. Robinson, J. L. Rognlien, C. K. Harnett, B. A. Simmons, C. R. B. Ellis, and R. V. Davalos, Bioelectrochemistry **69**, 117 (2006).
[25] C. Dietrich, M. Angelova, and B. Pouligny, J. Phys. II France **7**, 1651 (1997).
[26] M. Deserno and W. M. Gelbart, J. Phys. Chem. B **106**, 5543 (2002).
[27] J. Wang and M. Muthukumar, J. Chem. Phys. **135**, 194901 (2011).
[28] T. J. Willmore, *An Introduction to Differential Geometry* (Oxford University Press, New York, NY, 1959).
[29] M. Deserno, Phys. Rev. E **69**, 031903 (2004).
[30] Z. C. Tu and Z. C. Ou-Yang, J. Phys. A **37**, 11407 (2004).
[31] U. Seifert, Adv. Phys. **46**, 13 (1997).
[32] C. C. Fleck and R. R. Netz, Europhys. Lett. **67**, 314 (2004).
[33] W. Helfrich, Z. Naturforsch. **28**, 693 (1973).
[34] E. Evans, Biophys. J. **14**, 923 (1974).
[35] R. P. Rand, N. L. Fuller, S. M. Gruner, and V. A. Parsegian, Biochemistry **29**, 76 (1990).
[36] D. Marsh, Chem. Phys. Lipids **144**, 146 (2006).
[37] E. Evans and D. Needham, J. Phys. Chem. **91**, 4219 (1987).
[38] E. M. Lifshitz and L. P. Pitaevskii, *Physical Kinetics* (Pergamon, 1989).
[39] M. Muthukumar, J. Chem. Phys. **111**, 10371 (1999).
[40] C. W. Gardiner, *Handbook of Stochastic Methods* (Springer-Verlag, 1983).